Development of the 170GHz gyrotron and equatorial launcher for ITER

K.Sakamoto, A. Kasugai, K. Takahashi, R. Minami[a)], T. Kariya[b)], Y. Mitsunaka[b)], N.Kobayashi

Plasma Heating Laboratory, Japan Atomic Energy Agency (JAEA), 801-1Mukoyama, Naka-shi, Ibaraki, Japan 311-0193

Abstract. Recent progresses on the development of 170GHz gyrotron and an equatorial launcher are described. On the development of 170 GHz gyrotron, significant progress has been obtained. Up to now, stable 1 hour oscillation was demonstrated at the output power of 0.6 MW, which exceeds a discharge time of steady state experiment of ITER (3000 s). By optimizing the oscillation condition during the shot, the output power was enhanced up to 0.82 MW. The efficiency was 56 % with the depressed collector operation, and no trouble was found for 10min. The measured stray radiation in the gyrotron is 2 %, and the coupling efficiency with the corrugated waveguide is 96 %. In the design of the equatorial launcher, quasi-optical RF beam line was introduced. Consequently, the heat load on the movable mirrors due to the Ohmic loss of RF power was significantly reduced. These results give a clear prospect for an accomplishment of ITER ECH/ECCH system.

Email of K.Sakamoto: sakamoto.keishi@jaea.go.jp

1. Introduction

In ITER, the electron cyclotron heating and current drive system (ECH/ECCD) of 20 MW is planed [1]. As a power source of ECH/ECCD system, the developments of 1 MW/170 GHz gyrotron are underway at Russia [2], EU [3] and Japan. In JAEA (Japan Atomic Energy Agency), key technologies such as a demonstration of a depressed collector [4], demonstration of 170 GHz/1 MW oscillation at CW-relevant mode $TE_{31,8}$ [5], a success of the application of a synthetic diamond window [6-8], were carried out in ITER EDA (Engineering Design Activities). After ITER EDA, the pulse extension experiment has been continued, and 0.5 MW, 100 s was obtained in 2003 [9]. An improvement of built-in mode converter has been tried to reduce the stray radiation in the gyrotron in 2004. For CW operation, the cooling capability of the gyrotron test stand was enhanced in 2005. The electron beam current decreased during a shot due to the cathode cooling, a pre-program control of the heater power of the magnetron injection gun (MIG) was introduced (heater boost). These improvements enabled stable long pulse operations, 1000 s at 0.2 MW and 500 s at 0.3 MW [10]. In parallel, the oscillation experiment of a higher order volume mode, $TE_{31,12}$, at 170 GHz was carried out to study the feasibility of power enhancement. The cavity is cylindrical one, which gives an option of high order oscillation mode for long pulse higher power generation [11]. In this paper, the recent significant progress on the 170 GHz gyrotron for ITER and the updated design work of equatorial launcher are reported. In section 2, results of CW high efficiency 170GHz gyrotron development is described. In section 3, a design work for equatorial launcher is reported. Conclusion is given in section 4.

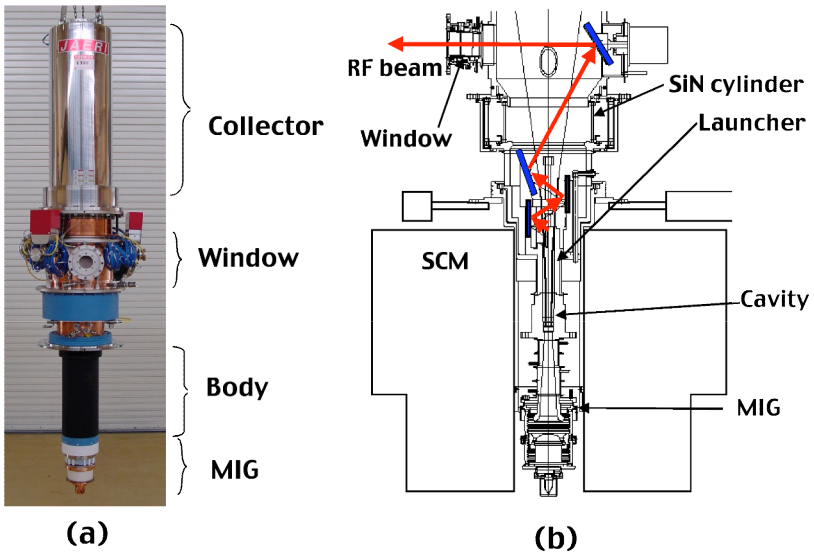

FIG. 1. (a) *Picture of 170GHz gyrotron (b) and the inner configuration.*

2. 170GHz Long Pulse Gyrotron

2.1. Configuration of 170GHz Gyrotron and Experimental Set-up

A picture of the 170 GHz gyrotron is shown in Fig.1(a), and the inner configuration is shown in Fig.1(b). The MIG is a triode. The oscillation mode is $TE_{31,8}$ at 170 GHz. The Q-factor of the cavity is 1530. The oscillation power is converted to the Gaussian beam by a built-in launcher and transported to the diamond window using four mirrors. An inner surface of the launcher is optimized to minimize a diffraction loss [13,14]. Fig.2 shows a radiation field distribution to the cylindrical surface at 60mm radius around the launcher. A rectangle in the figure denotes the area of the first mirror. A 99.5 % of the radiated power enters the first mirror. A stray radiation is extracted from a sub-window and from a ceramic insulator made of silicon nitride (SiN) between a body and a collector sections for the depressed collector operation. A 97.7 % of oscillation power is outputted from the diamond window. The collector is grounded. A positive voltage is applied to the body section for the depressed collector operation. In a long pulse operation, generally, some parameters change during the shot. For example, beam current decrease, oscillation frequency decrease due to the thermal expansion of the cavity, pitch factor of the rotational electron beam decrease. The time scale of these change are ~1min., 0.5sec, a few second, respectively. To compensate these change, heater power, magnetic field at the cavity (cavity field), anode voltage of the MIG are controlled during the oscillation. The output power couples with evacuated corrugated waveguide via two mirrors in matching optics unit (MOU). In the MOU, two-phase correlation mirrors are installed to couple with a HE_{11} mode at the input of the corrugated waveguide. The inner diameter of the waveguide is 63.5 mm, which will be adopted in ITER. In Fig.3, the photo of the transmission line is shown. The transmission line is composed of 7 m-waveguide, two-miter bends, a pre-dummy load and a 1 MW CW load. The transmission line was evacuated to suppress a breakdown.

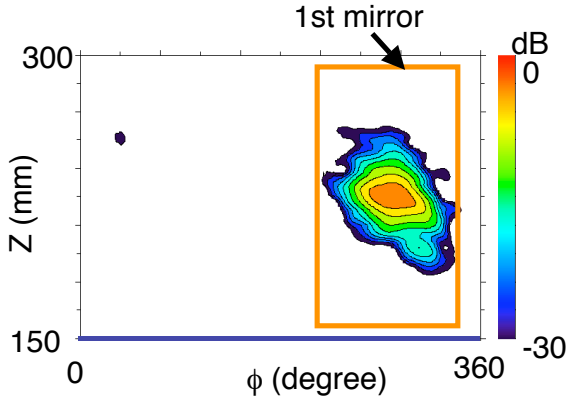

FIG. 2. A radiation field distribution to the cylindrical surface at 60 mm radius around the launcher. Rectangle denotes the area of first mirror.

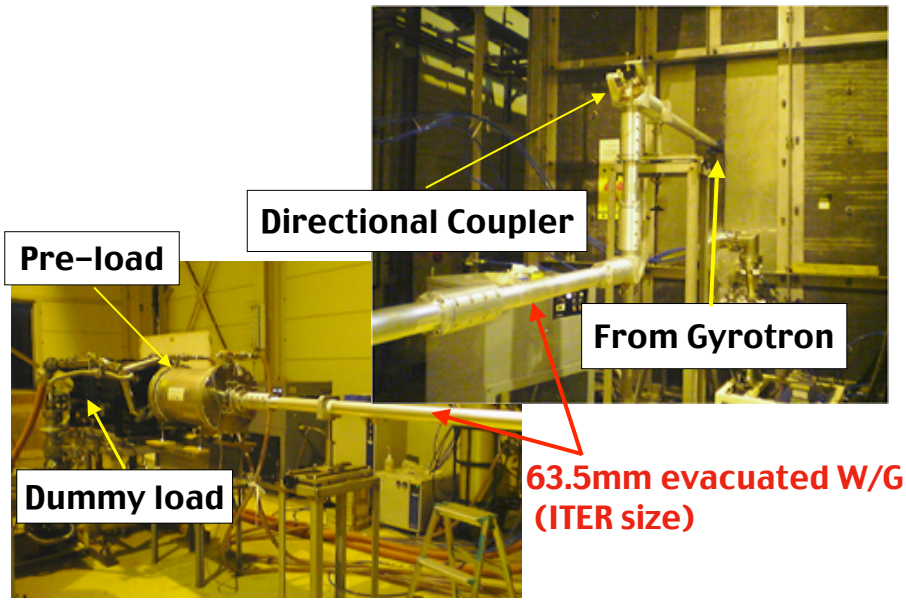

FIG. 3. Transmission line that connect the gyrotron and the dummy load. The transmission line composed of two miter bends, evacuated corrugated waveguide, pre-load and dummy load for 1 MW CW operation. Total length is ~7 m.

The waveguide comes out from the X-ray shield room inside which the gyrotron is installed. The power is measured calorimetrically from the temperature increase of cooling water of the dummy load and pre-load.

2.2. Short Pulse Experiment

Prior to the long pulse experiment, the gyrotron characteristics are studied at short pulse. The beam current dependence of output power and efficiency without the depressed collector is shown in Fig.4. The output power was measured by a dummy load made of silicon carbide, which was directly connected to the output window. The pulse duration was <1 ms, and the beam voltage was 72 kV.

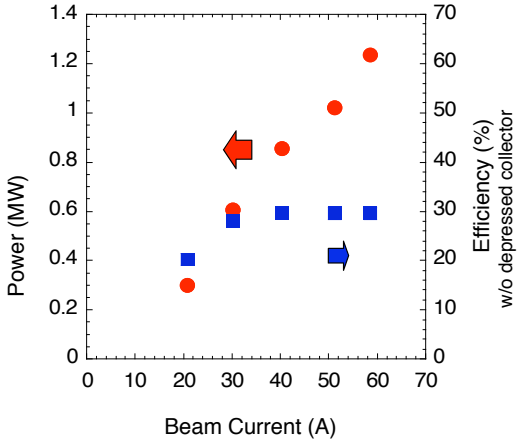

FIG. 4. Beam current dependence of output power and efficiency without depressed collector. Beam voltage is 72 kV, and pulse duration is ≤1 ms. Frequency is 170 GHz.

The detected frequency was 170 GHz. The oscillation power increase with the beam current and the output power exceeds 1 MW at the beam current I_c of ~49 A. In next, the depressed collector voltage was applied at the beam current I_c~49.5 A. Pulse duration was ≤26 ms. At the depressed collector voltage V_D=27 kV, overall efficiency reached at 51 % with the output power of ~1.12 MW.

2.3. Long Pulse Experiment

After the short pulse operation, the MOU was connected to the gyrotron as shown in 2.1. A pulse extension was carried out at the beam voltage of 72 kV, I_c~30 A, B_t=6.67 T. Fig.5 shows time traces of the depressed collector voltage, anode voltage, I_C, RF signal measured by a directional coupler, photo signal measured by a photo-multiplier from the viewing port of the gyrotron, a current of an 8 litter ion pump at the pulse duration of 3600 s. The output power at the gyrotron window is ~0.6 MW. The voltage of the main power supply was 44 kV. The overall efficiency with the depressed collector was 46 %. The RF power is identified from the temperature increases of the cooling water. All signals were stable. The vacuum pressure decreased after 40 min. The pulse duration is longer than that of the steady state experiment of ITER (3000 s). Fig.6 shows a conditioning process for pulse extension up to 1000 s. Within 10 days, the pulse was extended from 0.8 s to 1000 s at 0.6 MW output.

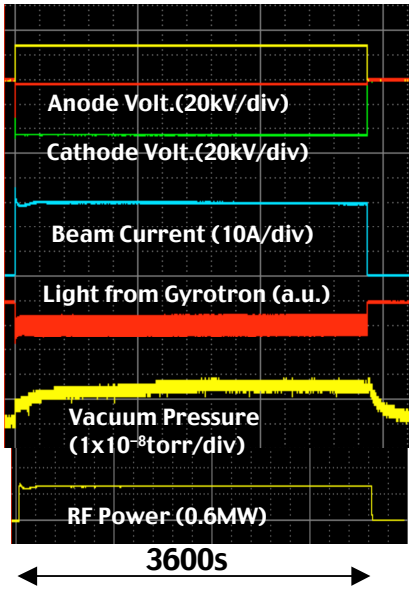

FIG. 5. Typical signals at long pulse operation of the gyrotron.

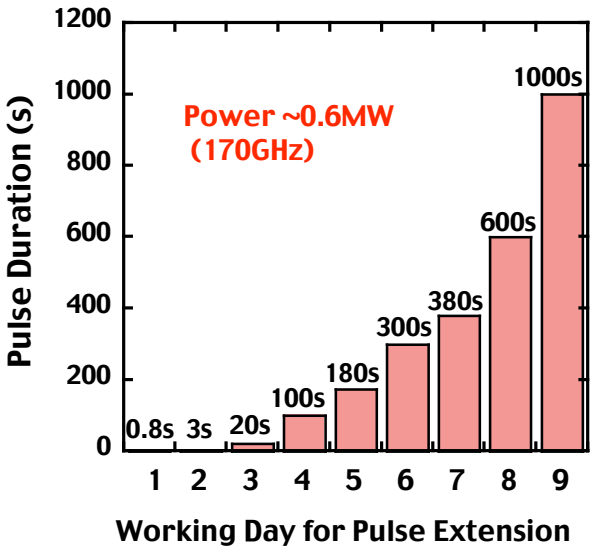

FIG. 6. Progress of pulse extension at initial phase of conditioning.

Fig.7 shows the RF power balance in case the transmitted power of 0.6 MW. In the MOU, the measured power dissipation is 25 kW, and loss in the transmission line estimated from the waveguide temperature increase is ~5 kW.

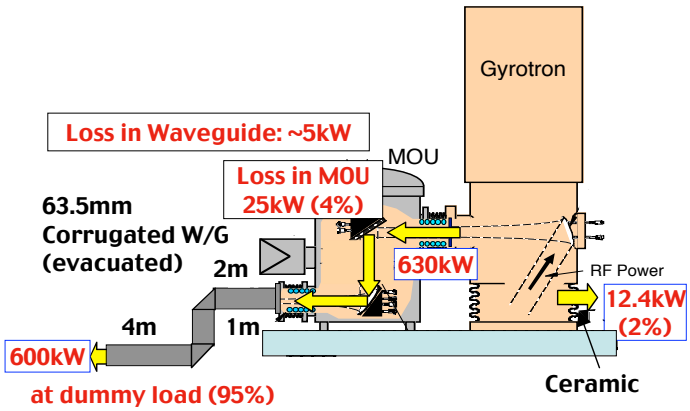

FIG. 7. Power balance of gyrotron and transmission line.

This indicates that the transmission efficiency to the dummy load via MOU, two miter bends and 7 m waveguides is 95 %, which gives a prospect for ITER transmission system. The stray radiation power coming out of the sub-window and the SiN cylinder is 12.4 kW (2 %).

2.4. Efficiency Enhancement

In the long pulse operation, the operation parameters are usually fixed. However, in CW operation, the operation parameters can be optimized during the oscillation in a finite time scale. In particular, in case of triode type MIG, there is an advantage that the pitch factor of the electron beam is controlled easily. With a combination of the cavity field control, the effective efficiency optimization is expected. Procedure to access the optimum parameter is as follows. The target mode is excited at proper parameters at first. This parameters need not to be an optimum. Next, the pitch factor and the cavity field are justified toward the optimum parameters during the shot keeping the target mode oscillation. With this active control method, the output power was significantly enhanced from 0.6 MW to 0.82 MW. The pulse duration was 10 min. The beam current and voltage were the same with those of 1hr operation shown in section 2.3. Consequently, the overall efficiency increased up to 56 %, which exceeds well the expected efficiency for ITER, 50 %. It should be noted that the efficiency is higher than that obtained in the short pulse operation as shown in Fig.4. One reason is the conditioning effect of the MIG. After the long pulse experiment, the efficiency has a tendency to increases compared with the initial stage. Another important reason is the optimization of the parameters is much easier that the short pulse operation in which a sensitive control of voltage start-up scenario is required to excite a desired high order mode. This method presents a possibility to avoid the mode competition problem and to realize a high efficiency oscillation at further higher mode.

3. Equatorial Launcher

In Fig.8, the reference design of the equatorial launcher is shown. The primary boundary of a transmission line is a tritium shield diamond window. The injection angles of three RF beam lines are controlled independently by three movable mirrors. The RF power is injected obliquely into the plasma for current drive. Onto the movable mirror, RF power is fed from 8 waveguides. A reference design is to transmit the RF power to the movable mirror using the waveguide array. One problem is that the peak heat load due to the RF loss on the movable mirror is relatively high ~3.2 MW/m^2. To reduce the heat load, quasi-optical transmission is proposed in the launcher. It is found the power density can be significantly reduced to less than 1.0 MW/m^2 by expanding the radius of each beam by adopting a quasi-optical transmission. In Fig.9 (a), the cross sectional view of the launcher (plane) is shown. The bundle of the waveguides was replaced to the empty space and the fixed mirror. The RF beams are radiated from the truncated corrugated waveguides toward the fixed mirror. Figs.9 (b) and (c) are the power distribution on the movable mirrors for waveguide transmission and quasi-optical one, respectively. These show the heat deposition to the movable mirror was averaged in the quasi-optical method and contributes to the reduction of the heat load. A simulation indicates the neutron flux at the window section is well below the critical value for the quasi-optical configuration. As for the R&D's of launcher components, neutron irradiation tests have been carried out for key components of a movable mirror, and reveal the applicability to ITER neutron environment [15]. And, the mock-ups of movable mirror, the tritium shield window, mirror supports and a controlling system of the movable mirror have been fabricated and tested. It was shown that these components would be feasible for the launcher.

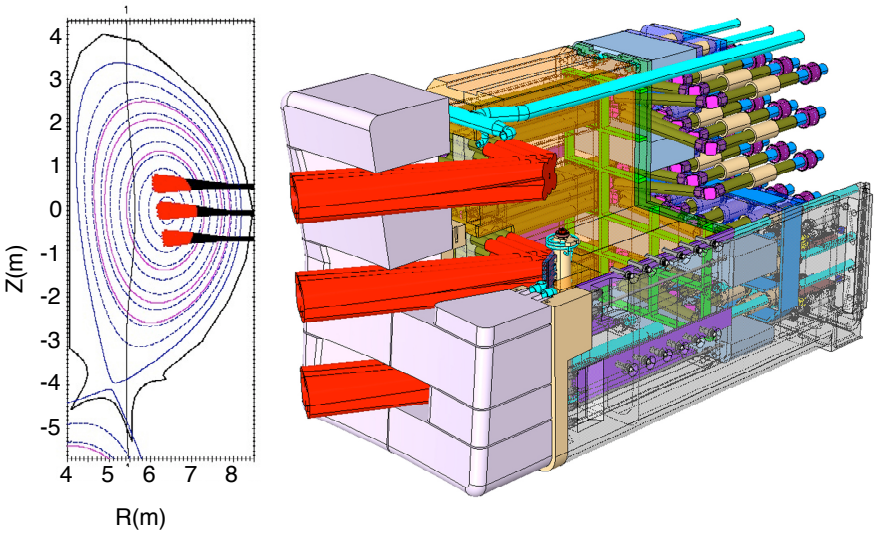

FIG. 8. Conceptual view of equatorial launcher and RF beams in the ITER plasma.

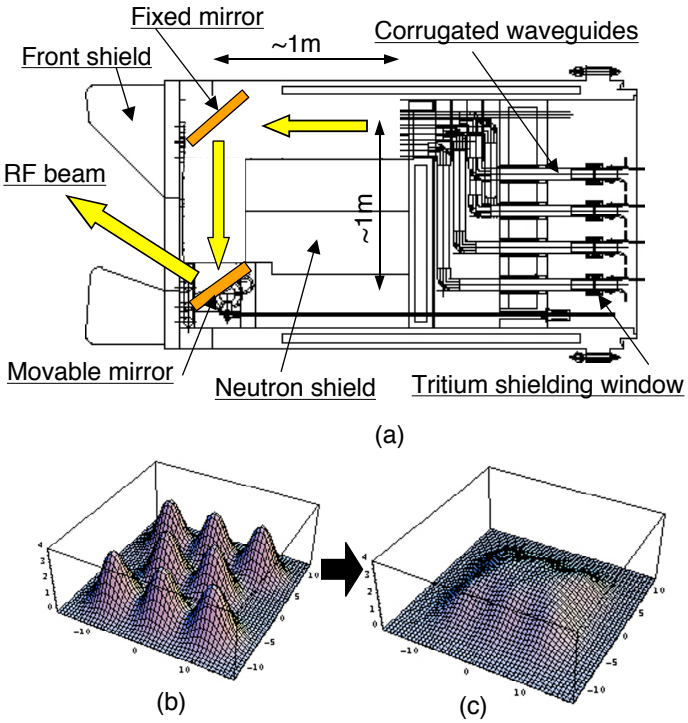

FIG. 9. (a) plane view of the equatorial launcher. The RF beams are radiated from the truncated corrugated waveguides and the flat RF distribution are formed on the mirrors. (b) The RF power distribution on the movable mirror for the waveguide transmission. (c) The RF power distribution for quasi-optical transmission.

4. Conclusion

The recent progress of 170 GHz gyrotron development in JAEA was described. The stable 1 hour oscillation was demonstrated at output power of 0.6MW with the overall efficiency of 46 %. These are significantly enhanced by the parameter optimization during the shot up to 0.82 MW and the efficiency of 56 % with the depressed collector. In the design work of equatorial launcher, the quasi-optical RF beam transmission was proposed, which significantly reduce the heat load due to the Ohmic loss on the mirrors in the launcher. These results give a clear prospect for accomplishment of ITER ECH/ECCD system.

Acknowledgments

We would like to thank to Dr.H.Takatsu, Dr.R.Yoshino and Dr.T.Tsunematsu for their encouragement.

a) Present address: Plasma research center, Tsukuba university,
Tennohdai, Tsukuba, Ibaraki, 305-8577 Japan.
b) Toshiba Electron tubes & devices co.,ltd, Ohtawara-shi, Tochigi, 324-8550 Japan.

References

[1] Technical Basis for the ITER Final Design Report (FDR), 2001.
[2] Litvak, A.G., et al., in Proc. IAEA Fusion Energy Conference 2004, FT/1-1Ra (2004).
[3] Piosczk,B., Dammertz,G., Dumbrajs,O., et al., J. of Physics:CS **25** (2005) 24.
[4] Sakamoto,K.,, Tsuneoka,M., Phys.Rev.Lett., **73**, (1994) 3532.
[5] Sakamoto,K., Kasugai,A., J.Phys.Soc.Jpn., **65**, (1996) 1888.
[6] Braz,O., Kasugai,A., Sakamoto,K., et al., Int.J.Infrared and millimeter Waves, **18**, (1997) 1495.
[7] Kasugai,A., Sakamoto,K., et al., Rev. Sci. Instrum, **69**, (1998) 2160.
[8] Sakamoto, K., Kasugai,A., et al., Rev. Sci. Instrum., **70**, (1999) 208.
[9] Sakamoto,K., Kasugai,A., et al., Nucl. Fusion, **43** (2003) 729.
[10] Kasugai,A., Minami, R.,et al., to be published in Fusion Eng. Des.(2006).
[11] Sakamoto,K., Kasugai,A., et al., J. of Physcs: CS **25** (2005) 8.
[12] Sakamoto, K., Takahashi,K., Kasugai,A., et al., Fusion Engineering and Design, **81** (2006) 1263.
[13] Neilson,J., IEEE Trans. Plasma Science, vol.34 (2006).
[14] Minami,R., Kasugai,A., et al., J.Infrared and mm waves, **27**, no.1 (2006) 14.
[15] Takahashi,K., Kobayashi,N., et al., J. of Physcs: CS **25** (2005) 75.